Control of the Electron Transfer Rate between Cytochrome c and Gold Electrodes by the Manipulation of the Electrode's Hydrogen Bonding Character

By: Haiying Liu, Hiromichi Yamamoto, Jianjun Wei and David H. Waldeck

H. Y. Liu, H. Yamamoto, J. Wei, and D. H. Waldeck, "Control of the Electron Transfer Rate between Cytochrome c and Gold Electrodes by the Manipulation of the Electrode's Hydrogen Bonding Character" *Langmuir*, 2003, 19(6), 2378-2387.

Abstract:

Oxidation and reduction of cytochrome *c* in solution through 11 different self-assembled monolayers (SAMs) on gold electrodes was investigated with cyclic voltammetry. Electron-transfer rate constants of cytochrome *c* through the 11 SAMs ranged from $\leq 10^{-4}$ to $\sim 10^{-1}$ cm/s. A strong correlation between the electron transfer rate constants and the hydrogen bonding ability of the SAM is identified. This correlation is discussed in terms of the dependence of the rate constant on the outer-sphere reorganization energy, the double layer, and the electronic coupling between the cytochrome and the differently terminated monolayer films.

Keywords: cytochrome *c* | self-assembled monolayers (SAMs) | electron transfer reactions | redox active protein | biosensors and biocatalytic devices | electrodes

Article:

I. Introduction

A number of workers are investigating electron transfer reactions with cytochrome *c*, to fully characterize this canonical example of a redox active protein, to clarify electron-transfer reactions in biological systems, and to aid in the development of biosensors and biocatalytic devices.[1,2] It has been difficult to determine the electron-transfer rate constant of the native cytochrome *c* by electrochemical methods because of preferential adsorption of impurities and the denaturated and/or oligomeric form of the protein that binds to the electrode.[3] Chemical control of the electrode surface can solve these problems, and many kinds of self-assembled monolayers (SAMs) have been developed as promoters.[4-6] The monolayer films on metal electrodes are composed of molecules with a basic structure of X−R−Y, where X is a group that can bind to the electrode (e.g., −SH, −S−, −S−S−, −P<, and R is a bridging unit (typically an alkane chain), and Y is a group that can interact with the redox couple in solution (e.g., **A**, $-NH_2$, and −COOH). Metal ions, e.g., $Mg^{2+}$and $Cr(NH_3)_6^{3+}$, have also been used to improve the attraction between the monolayer film and the protein. Despite this broad set of work, systematic studies that relate the electron-transfer rate constants to the hydrogen bond/electrostatic interactions with promoter SAMs is lacking.

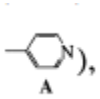

A),

The electron transfer between a redox couple and an electrode is often described by a nonadiabatic mechanism in which the electron tunneling probability is determined by a superexchange interaction.[7] The total electronic exchange interaction is often dominated by covalent, “through-bond”, contacts between the donor and acceptor. Nevertheless, it is well known that hydrogen bond contacts[8,9,10] and nonbonded contacts, “through space”,[11] can contribute significantly to the total electronic coupling between an electron donor and electron acceptor. Such findings are most well developed for intramolecular and intermolecular systems but are being elucidated for electron transfer between metal electrodes and redox couples. Recent studies have shown that the chemical composition of the molecules comprising a SAM film has an important impact on the electron tunneling probability, a finding that is in agreement with the superexchange model for the electron tunneling probability.[12] Other studies are demonstrating that noncovalent contacts can play a role in the electron transfer; for example, recent studies of the electron tunneling through alkanethiol monolayers show that the electronic interaction depends on the tilt-angle of the alkane chain with respect to the surface normal.[13] These findings can be understood as resulting from electron tunneling contributions that arise from nonbonded contacts, or “interchain” couplings.

Cytochrome *c* is an important respiratory redox protein that acts as an electron shuttle, or transporter.[1] In addition to the fundamental issues discussed above, it is important to clarify the relationship between the interactions of lysine groups ($-NH_3^+$) on cytochrome's exterior and its electron-transfer function.[14] The major function of cytochrome *c* is to transport an electron from complex III, containing cytochrome *b* and c_1, to complex IV, containing cytochrome oxidase (cytochrome *a* and *a*3) at the inner membrane where molecular oxygen is reduced into water.[1]Cytochrome *c* is a positively charged protein, because of lysine groups on its outer

surface, and can easily bind to the negatively charged cytochrome c_1 in complex III and cytochrome *a* in complex IV. Cytochrome *c* also transports an electron from other cytochromes (e.g., *b*, b_2, b_5) at the outer-, the inner-, and the intermembrane to cytochrome oxidase.[1] For these reasons, it is important to understand whether hydrogen bonding and electrostatic interactions between the cytochrome *c* and its redox partner is important for its redox chemistry.

This work investigates heterogeneous electron transfer rate constants of cytochrome *c* through 11 different SAMs (see Chart 1) that are of similar thickness but have very different terminal groups. That is, the chemical functionalities presented to the aqueous phase by the SAM are very different. The electron transfer rates were measured by cyclic voltammetry and were found to change by more than a 1000-fold in magnitude. The changes in the electron transfer rate constants were compared with empirically calculated Gibbs free energies for hydrogen bond complexation between the SAMs and the cytochrome *c*.[15] A significant correlation between the hydrogen bond interactions and the electron-transfer rate constants is identified for these model systems, implicating hydrogen bond formation as a significant actor in cytochrome *c*'s function.

II. Experimental Section

Chemicals. Horse heart cytochrome *c* (Sigma, type VI) was purified chromatographically in the manner described previously.[16,17] Fluorobenzoic acid (99%), 4-cyanobenzoic acid (98%), piperonyl acid (99%), and *N*,*N*'-dicyclohexylcarbodiimide (99%) were purchased from Alfa Aesar. 3-Furoic acid (99%) and DL-thioctamide (97%) **(11)** were purchased from Lancaster. ACS reagent grade disodium hydrogen phosphate, potassium dihydrogen phosphate, benzoic acid (99%), *p*-anisic acid (99%), monomethyl terephthalate (97%), *p*-toluic acid, isonicotinic acid (99%), and 4-(dimethylamino)pyridine (99%) were purchased from Aldrich. 2-Hydroxyethyl disulfide was obtained from Acros Organics. Water was purified with a Barnstead Nanopure system and had a nominal resistivity of 18 MΩ cm.

Bis[2-((4-cyanophenylcarbonyl)oxy)ethyl] Disulfide (7). DCC (2.86 g, 13.86 mmol) was added to a concentrated solution of 4-cyanobenzoic acid (1.86 g, 12.60 mmol), 2-hydroxyethyl disulfide (0.972 g, 6.30 mmol), and DMAP (0.154 g, 1.26 mmol) in 20 mL of dichloromethane at 0 °C. After 1 h the solution was allowed to warm to room temperature, and stirring was continued for 1 day. After removal of the precipitated dicyclohexylurea (DCU) by filtration, the product was recovered by extraction with CH_2Cl_2. After the CH_2Cl_2 extract was washed twice with water, it was dried with magnesium sulfate and then evaporated under reduced pressure. The disulfide bis[2-((4-cyanophenylcarbonyl)oxy)ethyl] disulfide was obtained by evaporation under reduced pressure and recrystallization with ethanol. The product was dissolved in methylene chloride and chromatographed on silica gel with methylene chloride. ^{1}H NMR (300 MHz) $CDCl_3$: δ 8.145 (d, *J*= 8.22 Hz, 4H), 7.7547 (d, *J* = 8.31 Hz, 4H), 4.638 (t, *J* = 6.48 Hz, 2H), 3.091 (t, *J* = 6.51 Hz, 4H). EI-HRMS: calcd 412.0562 ($C_{20}H_{16}N_2O_4S_2$), found 412.0552.

The disulfides below were prepared by a method analogous to that used for bis[2-((4-cyanophenylcarbonyl)oxy)ethyl] disulfide but used a different para-substituted benzoic acid reagent.

Bis[2-((phenylcarbonyl)oxy)ethyl] Disulfide (1). ^{1}H NMR (300 MHz) $CDCl_3$: 8.035 (d, *J* = 8.46 Hz, 4H), 7.534 (t, *J* = 7.47 Hz, 2H), 7.431 (t, *J* = 8.48 Hz, 4H), 4.599 (t, *J* = 6.56 Hz, 4H), 3.091 (t, *J* = 6.56 Hz, 4H). EI-HRMS: calcd 362.0642 ($C_{18}H_{18}O_4S_2$), found 362.0656

Bis[2-((4-methylphenylcarbonyl)oxy)ethyl] Disulfide (2). ^{1}H NMR (300 MHz) $CDCl_3$: 7.938 (d, *J* = 8.16 Hz, 4H), 7.234 (d, *J* = 8.10 Hz, 4H), 4.583 (t, *J* = 6.53, 4H), 3.087 (t, *J* = 6.56, 4H), 2.408 (s, 6H). EI-HRMS: calcd 390.0960 ($C_{20}H_{22}O_4S_2$), found 390.0965.

Bis[2-((4-fluorophenylcarbonyl)oxy)ethyl] Disulfide (3). ^{1}H NMR (300 MHz) $CDCl_3$: 8.0565 (q, *J* = 5.43 Hz, 4H), 7.099 (t, *J* = 8.69 Hz, 4H), 4.586 (t, *J* = 6.54 Hz, 4H), 3.078 (t, *J* = 6.48 Hz, 4H). EI-HRMS: calcd 398.0458 ($C_{18}H_{16}F_2O_4S_2$), found 398.0454.

Bis[2-((4-methoxyphenylcarbonyl)oxy)ethyl] Disulfide (4). ^{1}H NMR (300 MHz) $CDCl_3$: 7.990 (d, *J* = 8.82 Hz, 4H), 6.902 (d, *J* = 8.85 Hz, 4H), 4.558 (t, *J* = 6.52, 4H), 3.844 (s, 6H), 3.071 (t, *J* = 6.52, 4H). EI-HRMS: calcd 422.0858 ($C_{20}H_{22}O_6S_2$), found 422.0858.

Bis[2-((4-methoxycarbonylphenylcarbonyl)oxy)ethyl] Disulfide (5). ^{1}H NMR (300 MHz) $CDCl_3$: 8.098 (s, 8H), 4.629 (t, *J* = 6.525 Hz, 4H), 3.956 (s, 6H), 3.105 (t, *J* = 6.51, 4H). EI-HRMS: calcd 478.0751 ($C_{22}H_{22}O_8S_2$), found 478.0756.

Bis[2-((3,4-methylenedioxyphenylcarbonyl)oxy)ethyl] Disulfide (6). ^{1}H NMR (300 MHz) $CDCl_3$: 7.651 (d, *J* = 9.78 Hz, 4H), 7.462 (s, 2H), 6.827 (d, *J* = 8.19 Hz, 4H), 6.034 (s, 4H), 4.550 (t, *J* = 6.53, 4H), 3.061 (t, *J* = 6.51, 4H). EI-HRMS: calcd 450.0445 ($C_{20}H_{18}O_8S_2$), found 450.0443.

Bis[2-((4-pyridinylcarbonyl)oxy)ethyl] Disulfide (8). ^{1}H NMR (300 MHz) $CDCl_3$: δ 8.737 (d, *J* = 6.00 Hz, 4H), 7.799 (d, *J* = 6.03 Hz, 4H), 4.595 (t, *J* = 6.50 Hz, 4H), 3.052 (t, *J* = 6.51 Hz, 4H). EI-HRMS: calcd 364.0558 ($C_{16}H_{16}N_2O_4S_2$), found 364.0552.

Bis[2-((4-formylphenylcarbonyl)oxy)ethyl] Disulfide (9). ^{1}H NMR (300 MHz) $CDCl_3$: 10.105 (s, 2H), 8.203 (d, *J* = 7.8 Hz, 4H), 7.955 (d, *J* = 8.4 Hz, 4H), 4.649 (t, *J* = 6.60, 4H), 3.116 (t, *J* = 6.60, 4H). EI-HRMS: calcd 418.0552 ($C_{20}H_{18}O_6S_2$), found 418.0545. (It was prepared in a similar way without ethanol recrystallization).

DL-Thioctic-*N*-succinimidyl Ester (10). 10 was prepared according to ref 18.

Preparation of Self-Assembled Monolayers (SAMs) of the Disulfides. Gold wires (0.5 mm diameter, 99.99%) were boiled in 68% nitric acid overnight, removed from the nitric acid, and rinsed thoroughly (more than 10 times) with deionized water (>18 MΩ). The gold wire was heated in a natural gas/O_2 flame to form a ball of 0.08−0.12 cm^2 area and annealed in deionized water. The exposed wire was sealed in a glass capillary. The gold ball was reheated in the flame and then cooled in a stream of argon gas. Since it is known that the S−S bond of the disulfide is broken when a bond forms between the S atoms and the Au, the SAM[19]was formed by placing the electrode into a solution of ethanol and dichloromethane (1:1) that contained 1 mM disulfide for 2 days. The SAM modified electrodes were thoroughly rinsed with dichloromethane and water upon removal from the disulfide deposition solutions.

Electrochemical Measurements. Cyclic voltammetry was performed with an EG&G PAR-283 potentiostat that was controlled by a Pentium-466 PC running version 4.30 of PAR's M270 software and a GPIB board. A platinum wire auxiliary electrode and a Ag/AgCl (3 M NaCl) reference electrode, from BAS, were used in a three-electrode configuration with a working electrode. Gold electrodes modified with SAMs were used as the working electrode. All measurements were performed in a solution of 50 μM cytochrome *c* and 25 mM phosphate buffer at pH 7.0 under an argon atmosphere at room temperature. Impedance measurements (EIS) were performed in a three-electrode cell using a VoltaLab PGZ407 universal potentiostat to determine the capacitances of the SAMs and resistances of the 25 mM phosphate buffer solutions (pH of 7.0) containing cytochrome *c*. The resistances of the solutions containing cytochrome *c* were found to range from 10 to 300 Ω; the average and standard deviation values were 79 ± 79 Ω. The capacitances of the SAMs in the systems of **(4)** to **(11)** were 1.2 ± 0.6 $\mu F/cm^2$.

Calculation of the Molecular Lengths. The molecular lengths for the SAMs, discussed later, were calculated from a geometry optimized structure that was obtained by an MM+ molecular mechanics force field calculation, using Hyperchem 5.1. The lengths reported in Table 1 are evaluated between the furthest atoms: the S where the molecule links to the gold surface and the H on the end moiety (or the N in the pyridinyl moiety).

III. Results and Analysis

Chart 1 shows the molecular structures of 11 disulfide compounds **(1−11)** that were used to create SAMs on Au ball electrodes. Cyclic voltammograms were collected as a function of voltage scan rate for each of the SAMs. Figure 1 shows cyclic voltammograms of cytochrome *c* in solution for the SAMs composed of compounds **(4−11)** on gold electrodes at a voltage scan rate, *v*, of 20 mV/s. Cyclic voltammograms for the electrodes that were coated with SAMs of **1, 2,** and **3** did not show any faradaic peaks. Table 1 presents the apparent formal potentials $E^{0\text{‘}}$ and the parameter $|E_p - E_{p/2}|$ for the electrodes coated with SAMs of **4** through **11**. As can be seen in Table 1, the $E^{0\text{‘}}$ values of cytochrome *c* were observed to lie in the range from −1 to 10 mV versus Ag/AgCl. These $E^{0\text{‘}}$ values are intermediate between that observed for cytochrome *c* at hydroxyl terminated SAMs (69 mV)[20] and that for cytochrome *c* adsorbed on carboxylic acid terminated SAMs (−32 mV)[21]and are close to the $E^{0\text{‘}}$ of ∼30 mV versus Ag/AgCl reported for cytochrome *c* at 4-pyridinylthiol coated electrodes.[22] It is known that the formal redox potential of cytochrome is affected by interactions with extrinsic factors, e.g., the solvent and the electrode.[9,23]Recently, Whitesides and co-workers[24]suggested that the formal potential is affected by of the nature of the monolayer coating an electrode and its interaction with the adsorbed protein. However, the data obtained for the nonadsorbing case, reported here, does not show a clear trend, in part because of the error of ±2 mV in the $E^{0\text{‘}}$ determination and the small range of values from −1 to 10 mV. In contrast, a clear trend between the expected hydrogen bond interactions, using Gibbs free energy for hydrogen bond complexation between the cytochrome and the SAMs, and the observed electron-transfer rate constants can be identified (vide infra).

For the hydrophobically terminated SAMs of **1**−**3**, no faradaic response is discernible from the background current. Others[24,25] have reported that cytochrome *c* could be immobilized on alkanethiol monolayers, probably in a denatured form. The failure to observe a faradaic response indicates a very negative shift of the formal potential, outside of the voltage scan range in this work, and/or an electron-transfer rate constant that is very slow. In solution, the hydrophobicity of the layer could cause a larger average distance between the cytochrome *c* and the electrode surface, leading to a reduction in the electron-transfer rate constant. For example, incorporating a single hydration layer of H_2O between the cytochrome and the SAM is expected to cause a 10-fold reduction in the observed rate constant that would reduce the peak current by 10 times and result in a larger peak separation ΔE_p. It is possible to estimate an upper bound on the rate constant. If it is assumed that ΔE_p is 800 mV (the potential window of this study), the concentration of the cytochrome *c* at the surface is that of the bulk, and the systems **1**, **2**, and **3** are irreversible, then the electron-transfer rate constant k^0 is less than 10^{-6} cm/s.[26a]

Table 1 reports the values of $|E_p - E_{p/2}|$ for the SAMs of **4**−**11**. Most of the systems have $|E_p - E_{p/2}|$ values that lie between 56 and 70 mV for a scan rate of 20 mV/s. For a fully reversible system, the value of $|E_p - E_{p/2}|$ should be 56.5 mV. In contrast, the SAM of **10** has an $|E_p - E_{p/2}|$ value of 107 mV, which is much larger than that expected for a fully reversible system.[26] It is also evident that the SAM of **10** has the slowest rate constant and is the least likely to appear reversible. The change in peak shape for this system can be accounted for by consideration of the redox couple's quasi-reversible nature.

To understand and quantify the relative importance of mass transport to the electrode surface and the electron-transfer rate constant, one must solve the coupled diffusion and kinetics.[26c] The nature of the voltammogram (the peak current I_p, the peak potential E_p, and the half-peak potential $E_{p/2}$) can be characterized by the transfer coefficient α and the following unitless parameter

$$\Lambda = k^0(D_O^{1-\alpha} D_R^{\alpha}(nF/RT)v)^{-1/2} \qquad (1)$$

in which D_R is the diffusion constant of the reduced species, D_O is the diffusion constant of the oxidized species, n is the number of electrons transferred per species, k^0 is the apparent standard rate constant, and v is the scan rate. The parameter Λ provides a measure of the electron-transfer rate as compared to the redox species diffusion to the electrode and the voltage scan rate. Table 1 lists Λ for each of the systems at a scan rate of 20 mV/s.[27] The k^0 values were obtained by Nicholson's method,[28] as described later. As can be seen in Table 1, the SAMs composed of **8**, **9**, and **11** have values of Λ that are greater than 10, indicating that they behave reversibly at this scan rate. The systems **4**−**7** have values of $\Lambda \approx 1$, and that of **10** is $\Lambda \approx 0.1$, suggesting a deviation from the reversible-like behavior even at this small scan rate.[29] When the system is completely irreversible, the peak current is proportional to the square root of the voltage scan rate, but the value of $|E_p - E_{p/2}|$ is given to be $47.7/(\alpha n_a)$ at 25 °C, where n_a is the effective number of electrons in the rate-determining step.[26] If $\alpha = 0.5$ and $n_a = 1$, then the value of $|E_p - E_{p/2}|$ is 95.5 mV, which compares reasonably well for the case of SAM **(10)**.

Chart 1. Molecular Structures of the Disulfides Used in This Study

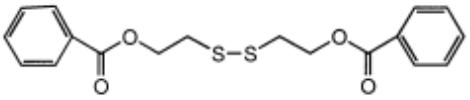

(1) bis[2-((phenylcarbonyl)oxy)ethyl]disulfide

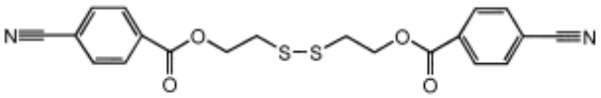

(7) bis[2-((4-cyanophenylcarbonyl)oxy)ethyl]-disulfide

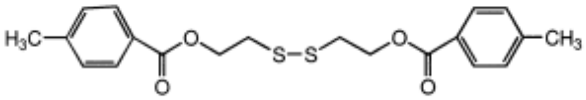

(2) bis[2-((4-methylphenylcarbonyl)oxy)ethyl]-disulfide

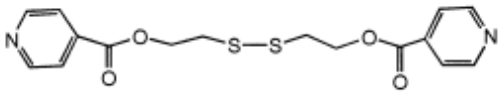

(8) bis[2-((4-pyridinylcarbonyl)oxy)ethyl]-disulfide

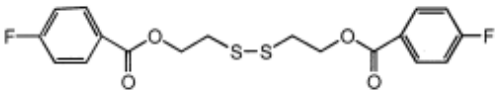

(3) bis[2-((4-fluorophenylcarbonyl)oxy)ethyl]-disulfide

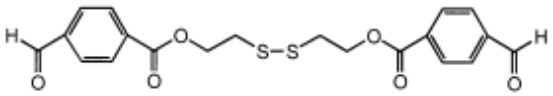

(9) bis[2-((4-formylphenylcarbonyl)oxy)ethyl]-disulfide

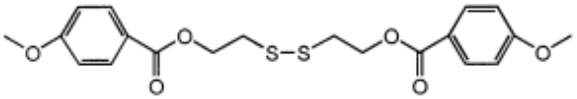

(4) bis[2-((4-methoxyphenylcarbonyl)oxy)ethyl]-disulfide

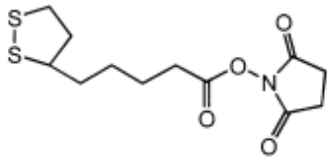

(10) DL-thioctic-N-succinimidyl ester

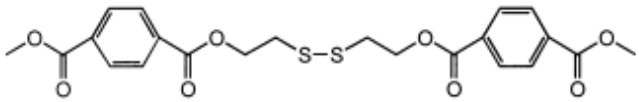

(5) bis[2-((4-methoxycarbonylphenylcarbonyl)oxy)-ethyl]disulfide

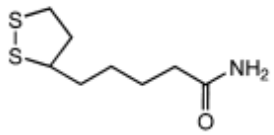

(11) DL-thioctamide

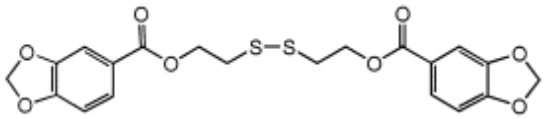

(6) bis[2-((3,4-mthylenedioxyphenylcarbonyl)oxy)-ethyl]disulfide

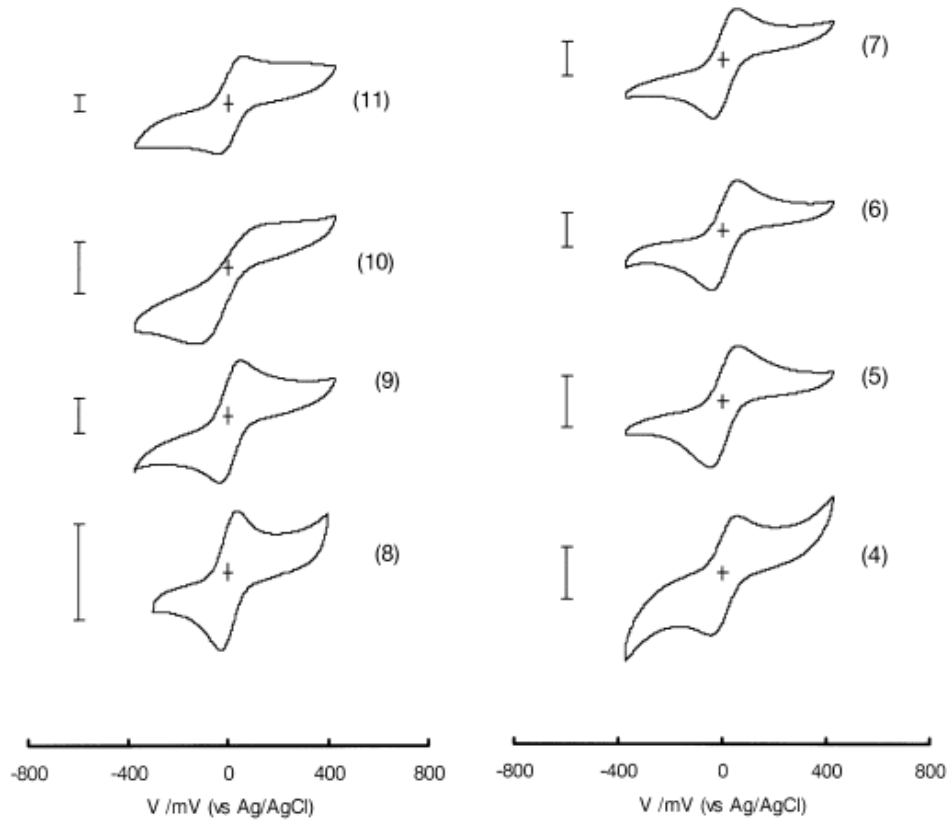

Figure 1. Cyclic voltammograms are shown for 50 μM cytochrome *c* in 25 mM phosphate buffer solution at pH 7, using the SAMs of **4**−**11** on gold electrodes. The scan rate is 20 mV/s. The lengths of the bars indicate a scale of 200 nA, and the crosses mark the origin. Cyclic voltammograms for the SAMs of **1**, **2**, and **3** did not show any peaks.

Table 1. Apparent Formal Potentials ($E^{o\prime}$), Standard Electron Transfer Rate Constants (k^0), the Parameter Λ, and Calculated Molecular Lengths (L) for the Different SAMs

	$E^{o\prime}$ [a]	$\lvert E_p - E_{p/2}\rvert$ [a]	$\log(k^0)$ [b]	Λ	L [c]
R_1−Ph (**1**)					0.91
R_1−Ph−OMe (**4**)	−1	57	−3.38 ± 0.47	0.9	1.10
R_1−Ph(CO)OMe (**5**)	5	70	−3.03 ± 0.09	1.6	1.23
R_1-benzodioxole (**6**)	3	68	−2.84 ± 0.06	2.5	0.99
R_1−PhCN (**7**)	7	65	−2.75 ± 0.01	2.9	1.09
R_1−Py (**8**)	5	56	−1.87 ± 0.56	49.9	0.90
R_1−PhCHO (**9**)	9	61	−1.80 ± 0.07	26.2	1.09
R_2−CO−O−succinimide (**10**)	−6	107	−3.96 ± 0.04	0.2	1.17
R2−CONH2 (**11**)	10	62	−0.96 ± 0.04	181.3	0.89

[a] The units are mV and $\lvert E_p - E_{p/2}\rvert$ is determined at a scan rate of 20 mV/s. The values of $\lvert E_p - E_{p/2}\rvert$ were measured from the oxidation peaks. The errors of the $E^{o\prime}$, E_p, and $E_{p/2}$ are ±2 mV. [b] The units of k^0 are cm/s and it is log base ten. [c] The units of L are in nm.

Scan Rate Dependence. The scan rate dependences of the cyclic voltammograms were studied for each system. Figure 2 presents cyclic voltammograms for electrodes coated with the SAMs of**5** and **8** in contact with 50 μM cytochrome *c*, at v = 20 and 600 mV/s, representing the cases of $\Lambda \approx 1$ and $\Lambda \geq 10$. The background current was subtracted from these data to better illustrate the

peak behavior with scan rate. As can be seen in Figure 2, the peak currents for **5** and **8** increase with an increase in the scan rate, and the peak positions shift apart. The peak currents in the systems of **4**–**9**, and **11** with the values of $\Lambda \geq 1$ were found to be proportional to the square root of the scan rate, which indicates that these systems are controlled by diffusion of cytochrome *c* in solution.[26] The SAM composed of **10** did not respond in this well-behaved manner, which will be discussed later. Details of this analysis are provided in the Supporting Information.

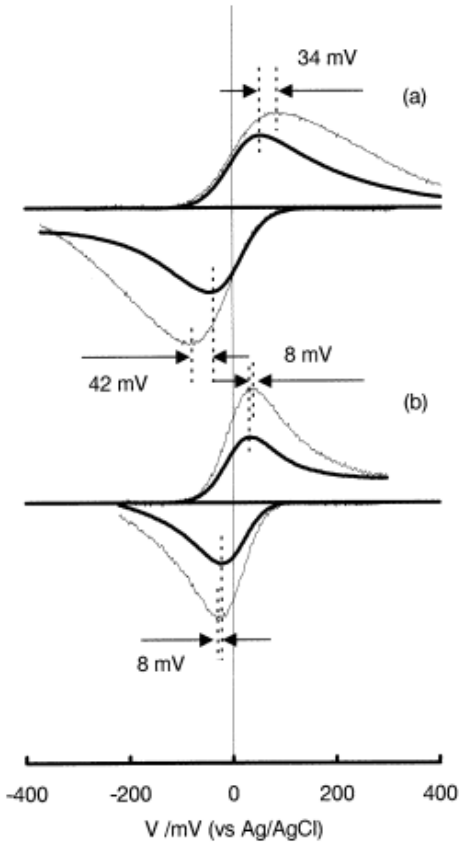

Figure 2. Cyclic voltammograms are shown for a 50 μM solution of cytochrome *c* through the SAMs of (a) **5** and (b) **8** between the scan rates 20 (bold line) and 600 (thin line) mV/s. The currents at 20 mV/s for **5** and **8** were multiplied by 2 and 3, respectively, for comparison. The backgrounds were subtracted.

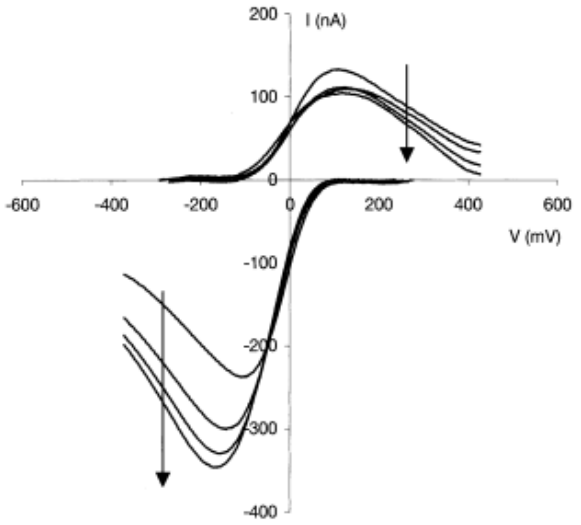

Figure 3. Cyclic voltammograms are shown for a 50 μM solution of cytochrome *c* through SAMs of **10** at scan rates of 20−80 mV/s. The arrows show the scan rates from 20 to 80 mV/s. The backgrounds were subtracted.

The observed peak potential E_p shifts with scan rate because the electron-transfer reaction becomes less reversible as the scan rate increases.[29,30] This effect may be appreciated by considering the case where the scan rate is faster than the electron-transfer rate. In this instance, the potential of the electrode passes by the E^{0}‘ more rapidly than the relative concentrations of the reactant and product can change to maintain equilibrium. In general, the observed peak potential depends on the relative values of the scan rate and the electron-transfer rate, and smaller electron-transfer rates result in larger peak separations at a given scan rate. In Figure 2, the voltammograms for the SAM of **8**, with a Λ value of 49.9, show a small shift of 8 mV. On the other hand, the cyclic voltammograms for the SAM of **5**with the Λ value of 1.6 has a peak shift of 34 mV for the oxidation peak and 42 mV for the reduction peak. Qualitatively, it is evident that the electron transfer of cytochrome *c* through **8** is much faster than that through **5**. It

is important to design the electrode configuration so that potential drops from nonfaradaic processes are minimized. The effect of the voltage drop arising from the solution resistances on the observed potential is found to be negligible, based on the average solution resistance of 79 Ω described in the Experimental Section. Honeychurch and Rechnitz[31] investigated the impact of the SAM properties on the cyclic voltammograms, under the assumption of no significant interaction between electroactive molecules and the monolayer. They found that the potential at the top of the monolayer depends on the potential of zero charge of the electrode, the amount of charge on the monolayer, and the capacitances of the film and the diffuse layers. This effect becomes significant when the capacitance of the monolayer exceeds 5 μF/cm^2, resulting in a shift of the peak potential. In this study the capacitances of the SAMs were kept below 2 μF/cm^2 to minimize such effects.

Figure 3 shows cyclic voltammograms for the SAM of **10** at scan rates ranging from 20 to 80 mV/s. The background current was subtracted from these data. As can be seen in Figure 3, the reduction peak current increases with the increase in scan rate, and it is found to be proportional to the square root of the scan rate (see the Supporting Information). The value of $|E_p - E_{p/2}|$ is independent of the scan rate and lies between 104 and 115 mV (average = 110 mV) however. In contrast, the oxidation peak current decreases from 132 to 103 nA, and the value of $|E_p - E_{p/2}|$ increases from 107 to 170 mV as the scan rate increases from 20 to 80 mV/s. This large deviation from the reversible-like behavior is consistent with the small value of $\Lambda \approx 0.1$ for the SAM of **10** and indicates quasi-reversible behavior for the electron transfer of cytochrome *c* through the SAM of **10** at these scan rates. Furthermore, the asymmetric behavior indicates that the deviation from the reversible-like behavior is larger for oxidation than for reduction; i.e., the electron-transfer rate for the oxidation is slower than that for the reduction.

For all of these SAMs, the cytochrome *c* was not immobilized on the surface. As described above, the electron-transfer rates in these systems are controlled by diffusion of cytochrome *c* in solution, as judged from a plot of the peak current versus the square root of the scan rate. In addition, after the voltammetry measurements were performed in the cytochrome *c* solutions, the electrodes were immediately placed in a blank buffer solution and the current−voltage scans did not show any faradaic response. Together, these results provide compelling evidence that the cytochrome does not adsorb to the surface for time scales longer than the characteristic time of electron transfer.

Obtaining k^0. The change in ΔE_p with scan rate can be used to quantify the standard heterogeneous electron-transfer rate constant k^0, using Nicholson's method.[26,28] To describe the deviation from equilibrium, Nicholson solved the diffusion-reaction equations for triangular potential waves ($E(t) = E_i - vt$) like those used in cyclic voltammetry. He numerically calculated the change in peak separation ΔE_p as a function of the system parameters. A table of ΔE_p as a function of the reduced rate constant is given in ref 28 and was used to determine the k^0 values. Table 1 presents the logarithm of k^0 for cytochrome *c* through the SAMs **4**−**11**. The analysis assumes that the transfer coefficient α is 0.5 and the diffusion constants for the reduced and oxidized cytochrome are the same, $D_R \sim D_O = 4.7 \times 10^{-7}$ cm^2/s.[20] Note that the k^0 values of cytochrome *c* for **8** and **11** are about 1000 times faster than that for **4** and **10**.

A number of factors determine the standard electron-transfer rate constant at the coated electrode, including the film thickness, chemical composition and structure of the SAM, and the affinity between the SAMs and the cytochrome. Walton and co-workers[5a] reported k^0 values of horse heart cytochrome *c* in solution using more than 50 surface modifiers containing compounds related to pyridine, aniline, carboxylate, phosphate, sulfonate, and so forth. They identified four classes of behavior: I, no response; II, $k^0 \leq 10^{-4}$ cm/s; III, 10^{-4} cm/s $\leq k^0 \leq 10^{-3}$ cm/s; IV, $k^0 \geq 10^{-3}$cm/s. Walton et al.[5a] rationalized these behaviors with pK_a values and molecular conformations of the promoters qualitatively but did not attempt to quantitatively compare the electron-transfer rate constants with the hydrogen bond interactions. As can be seen from Table 1, the SAMs of **5**−**9** and **11** would be categorized in class IV, while the SAM of **4** lies in class III, and the SAM of **10** lies in class II.

It is well-known that the distance between the electrode and the cytochrome in solution can affect the electron-transfer rate constant. It is believed that there are two regimes in the electron-transfer mechanism, i.e., adiabatic (a strong electronic coupling) and nonadiabatic regimes (a weak electronic coupling).[30,32] If the electron-transfer belongs to the adiabatic regime, then the distance dependence of the rate constant is negligible.[30,32] If the electron-transfer lies in the nonadiabatic region, the electron-transfer rate constant would decrease by about one-third for each angstrom change in the film thickness.[7] Since the adiabatic and nonadiabatic regimes depend on the electron-transfer distance,[32] it is important to know the electron-transfer regime for the minimum electron-transfer distance in this study.

Table 1 lists the calculated molecular lengths for each of the SAMs of **4**−**11**. The lengths range from 8.9 Å for **11** to 12.3 Å for **5**, and the average length is 10.2 ± 1.3 Å. Since the effect of the π structure on the phenyl groups in the SAMs of **4**−**9** should enhance "through-bond" interactions,[33]the effective electron-transfer distances for the systems **4**−**9** would be shorter than the physical distances and makes the lengths more comparable to that of **10** and **11**. When an electron-transfer distance of 5 Å in cytochrome *c*[34] and a distance of 2 Å between the end sulfur of the SAMs and the substrate[7b] are added to the average molecular lengths of 10 Å, the minimum electron-transfer distance in this study should be around 17 Å, which may be in the intermediate regime between the adiabatic and nonadiabatic limit.[32] With the reported electron tunneling decay factor $\beta = 1.07$ Å^{-1},[21,32,35] it is predicted that the electron-transfer rate constant changes by 40-fold in magnitude with a variation of 3.4 Å in the electron-transfer distance, the maximum difference in physical lengths reported in Table 1. It is also apparent from the lengths and rate constants that the variations are not well correlated. Therefore, the 1000 times difference in the rate constants from **4** to **11** cannot be explained by a simple distance effect, and the electron-transfer rate-determining factors must involve the interaction between the cytochrome *c* and the SAMs.

IV. Discussion

The apparent electron-transfer rate constant k^0 is influenced by a number of system parameters. It is known that the intrinsic electron-transfer rate constant k_{et}^0 at the formal potential $E^{0\prime}$ in the adiabatic limit is determined by the reorganization energy λ_o and the characteristic polarization relaxation time τ_{eff} of the solvent and protein interior, whereas that in the nonadiabatic limit is determined by the reorganization energy λ_o and the electronic coupling between electron donor

and acceptor $|V|$.[36] Since the solvent composition is common in this study, the τ_{eff} should be similar between systems. One might expect local changes in the solvent structure near the SAM surface; however these are unlikely to cause a 1000-fold change in the polarization relaxation time. For a system in which the redox molecule is present in bulk solution and is transported to and from the electrode surface, the apparent standard rate constant k^0 can be conveniently written using the "encounter/pre-equilibrium" approximation[37] so that

$$k^0 = k_{et}{}^0 K \qquad (2)$$

K is viewed as an equilibrium constant that describes the concentration of the reactant in the reaction zone with an effective thickness δR_e and can be written as

$$K = \delta R_e \exp\left(-\frac{ZF\Phi_r}{RT}\right) \qquad (3)$$

where Z is the effective charge of the cytochrome and Φ_r is the effective potential at the average distance of electron transfer (usually taken to be the outer Helmholtz plane). This potential is likely to be strongly influenced by the chemical nature of the SAM surface and the electrolyte solution. Variations in the three parameters, λ_o, K, and $|V|$, with the terminal unit of the SAMs are the likely causes of the rate constant differences. Assuming that the change in the apparent rate constant arises from changes in the activation free energy, a 1000-fold change of rate constant requires 0.198 eV (or 17.1 kJ/mol) change in the activation energy, ΔG_{act}.[38] This 200 meV energy shift could arise from the change in the effective potential (eq 3) and would be determined by the change in the SAM terminal group.

In contrast, the change in the apparent rate constant could arise solely from changes in the intrinsic rate constant. In this case it is possible to estimate the required changes in the solvent reorganization energy and/or the electronic coupling for the different SAM coated electrodes. Given the large distance of more than 17 Å for the electron transfer, the electron transfer is taken to lie in the nonadiabatic regime, or near it.[32] In this limit, the intrinsic standard rate constant $k_{et}{}^0$at the formal potential $E^{0\text{‘}}$ can be written, as[7,32]

$$k_{et}{}^0 = \frac{|V|^2}{\hbar}\rho_m\left(\frac{\pi^3 RT}{\lambda_o}\right)^{1/2}\exp\left(-\frac{\Delta G_{act}}{RT}\right) \qquad (4)$$

where ρ_m is the density of electronic states in the electrode, and the activation free energy is given by

$$\Delta G_{act} = \frac{\lambda_o}{4} - |V| \qquad (5)$$

From eq 5 and assuming that $|V| \ll \lambda_o$, which is consistent with the assumption of nonadiabaticity, a 1000-fold reduction in the rate constant requires a 0.7 eV change in the reorganization energy ($(\lambda_o)_{1000} \approx (\lambda_o)_1 - 0.685$ in eV, where the subscript on (λ_o) indicates the relative change in the rate constant). When $(\lambda_o)_{1000}$ = 0.7 eV, the 1000-fold reduction in the rate

constant can result from a 2-fold enhancement in the reorganization energy. Alternatively, one might assign the entire rate constant change to the change in $|V|$. If the λ_o is not changed, the 1000-fold drop in the rate constant requires a 32-fold reduction in $|V|$.

It is known that the reorganization energy is comprised of inner- and outer-sphere components.[36]Because the inner-sphere reorganization energy, associated with the heme, for cytochrome *c* is small (≤0.03 eV),[39] the discussion focuses on the outer-sphere reorganization energy, which is affected by the dielectric constant of solvent and the protein shell.[40] Since the dielectric constant of water at the liquid−solid interface region is different from the bulk value,[41] the reorganization energy in the interface region should also change from that in the bulk. For the case of an aqueous solution, a hydrophobic SAM surface is found to reduce the polarity of solvent, while a hydrophilic surface enhances the polarity.[41a] Liu and Newton[42] used a continuum model to predict the outer-sphere reorganization energy at three component (electrode, SAM, liquid) interfaces. They reported that the outer-sphere reorganization energy depends on the size of redox species, the distance of the redox species from the top of the SAM on the electrode, the SAM thickness, and the dielectric constants of solvent, film, and the electrode. Using their result, one can predict the change in the reorganization energy. If the dielectric constant varies by ±30 from the value of 80 for the bulk water,[43] the reorganization energy changes very little, from 0.61 eV for a dielectric constant of 50 to 0.63 eV for a dielectric constant of 110, at a film thickness of 12 Å (see ref 42 for more details). A more important effect is the variation of the reorganization energy with film thickness. At an average thickness of 12 Å, a ±2 Å variation causes a deviation of ±0.02 eV in the reorganization energy. In addition, the hydrophobic surface reduces the reorganization energy, whereas the hydrophilic surface increases the reorganization energy. This trend is opposite to that observed experimentally. From these considerations, the 1000-fold enhancement in the rate constant is unlikely to be caused by a change in the reorganization energy, which can arise from a change in effective dielectric constant near the SAM surface.

The electronic coupling term's distance dependence is well characterized by $|V| = |V_0| \exp(-\beta r/2)$, where $|V_0|$ is the electronic coupling matrix element at the minimum electron donor−acceptor separation distance (defined as $r = 0$), β is the electron tunneling decay factor, and r is the electron donor−acceptor distance. Since k_{et}^0 is proportional to $|V_0|^2 \exp(-\beta r)$, the electronic coupling interactions are very sensitive to the electron donor−acceptor distance. However, as discussed above, the variation of film thickness alone cannot explain the 1000-fold enhancement in k^0. Hydrogen bonding interactions have been linked to electron-transfer efficiency in other studies. Beratan et al.[44] have proposed the use of electron transfer pathways for proteins in the nonadiabatic regime and determined how different interactions, namely covalent bonds, hydrogen bonds, and through-space interactions, contribute to the electron transfer. Sek et al.[45a] also reported an enhancement of electron transfer rate constants for alkanethiol chains that contain an amide moiety and ascribed it to a hydrogen bond network that links the chains together and increases the efficiency of electron transfer pathways. It is believed that positively charged lysine groups ($-NH_3^+$) on the cytochrome *c* periphery facilitate electrostatic and hydrogen bonding interactions with some SAMs,[3-6] and it has been recognized that the orientation of cytochrome *c* at the surface is an important factor for electron transfer from cytochrome *c*.[3-6] In fact, the distance from the iron in the heme to the edge of the heme that is exposed to the cytochrome's surface is 7 Å, whereas those from the iron to hydrophobic residues

Proline 44, Proline 76, Isoleucine 57, and Valine 3 on the horse cytochrome *c*'s surface are 16−20 Å.[46] Clark and Bowden[21e] reported that the electron-transfer rate constant depends on the adsorption state of the cytochrome *c*. From the above considerations, it is evident that the electronic coupling strength between the cytochrome and the electrode will depend on the orientation of the cytochrome *c* at the surface, because it changes the heme's distance from the electrode. The orientation of the cytochrome from the surface will depend on the hydrogen bond interactions between the cytochrome periphery and the SAM. Because it was demonstrated that the interaction between the cytochrome and the SAM does not immobilize the protein, we suggest that the electrostatic and hydrogen bond interactions act to orient the protein or to pull the protein's redox active heme closer to the surface and improve the electron-transfer efficiency.

If the hydrogen bond interactions between the cytochrome and the SAMs of **4**−**11** are determining the cytochrome's surface proximity, then a quantitative measure of this interaction should correlate with the electron-transfer rate constants shown in Table 1. The model discussed below is used to quantify the strength of the hydrogen bond interactions between the cytochrome and the SAMs. Assume the following reaction for formation of a cytochrome to SAM hydrogen bond

$$\mathrm{Cyt{-}NH_3^+{\cdots}OH_2 + H{-}O{-}H{\cdots}SAM \rightleftharpoons Cyt{-}NH_3^+{\cdots}SAM + 2H_2O} \quad (6)$$

where Cyt−$NH_3^+\cdots OH_2$ is hydrated cytochrome *c*, H−O−H···SAM is hydrated SAM, and the Cyt−$NH_3^+\cdots$SAM is an adduct formed between cytochrome *c* and the SAM. This net reaction can be decomposed into the following three equilibria

$$\mathrm{Cyt{-}NH_3^+ + SAM \overset{K_1}{\rightleftharpoons} Cyt{-}NH_3^+{\cdots}SAM} \quad (7)$$

$$\mathrm{H_2O + SAM \overset{K_2}{\rightleftharpoons} H{-}O{-}H{\cdots}SAM} \quad (8)$$

$$\mathrm{Cyt{-}NH_3^+ + H_2O \overset{K_3}{\rightleftharpoons} Cyt{-}NH_3^+{\cdots}OH_2} \quad (9)$$

where K_i (i = 1, 2, 3) is the equilibrium constant in each case. Abraham and co-workers[15] have developed an empirical method to predict the equilibrium constants for acid−base adduct formation. The equilibrium constant K is given by

$$\log K = 7.354\alpha_2^{\mathrm{H}}\beta_2^{\mathrm{H}} - 1.094 \quad (10)$$

where α_2^{H} and β_2^{H} parameters are obtained by the following equations

$$\alpha_2^{\mathrm{H}} = (\log K_{\mathrm{A}}^{\mathrm{H}} + 1.1)/4.636 \quad (11)$$

and

$$\beta_2^{H} = (\log K_B^{H} + 1.1)/4.636 \qquad (12)$$

The values of log K_A^H for acids are statistical parameters that are obtained by fitting the log *K*values for a series of acids against reference bases. Correspondingly, the values of log K_B^H for bases are obtained by fitting the log *K* values for a series of bases against reference acids. The parameters of α_2^H and β_2^H have been reported for more than 300 acids and 200 bases.[15]

By use of eqs 10−12 and the parameters α_2^H and β_2^H from ref 15, the Gibbs free energy change ΔG for the equilibria 7 to 9 can be found via $-\Delta G = RT \ln(K)$. Table 2 presents Gibbs free energy changes ΔG_1 and ΔG_2 for the equilibria in eqs 7 and 9. Table 3 lists the parameter values for compounds whose functionalities correspond to the end moieties of the SAMs used in this study, i.e., pyridine, 1,4-dioxane, cycloalkanes, RCOOR, Et−NH_2, $MeCONMe_2$, and Ph−R, where Ph is a benzene, and R = −OMe, −CO−OMe, −CN, and CHO. The binding to the cytochrome *c* was assumed to occur through the lysine group (−NH_3^+), whose pK_a value was taken to be 10.1.[47] A Gibbs free energy change ΔG_3 for the equilibrium in eq 9 was determined from the parameters in Table 3 and found to be −3.6 kJ/mol. The net Gibbs free energy change $\Delta(\Delta G)$ for the equilibrium 6 is given by

$$\Delta(\Delta G) = \Delta G_1 - \Delta G_2 - \Delta G_3 \qquad (13)$$

Figure 4 shows a plot of log(k^0) versus $-\Delta(\Delta G)$ for the SAMs of **4−11**. The correlation coefficient for a linear fit to these data is found to be 0.92, if the **10-2** point is excluded. This correlation strongly suggests that the standard electron-transfer rate constants k^0 for the cytochrome *c* is associated with the hydrogen bond interactions between the cytochrome *c* and the SAMs. As can be seen in Figure 4, the point of **10-1**, obtained by the parameters of cycloalkanes, correlates well with the linear fitting, but that of **10-2**, obtained by those of RCOOR, does not. The geometry optimization of compound **10** revealed a bent molecular structure, resulting from interactions between the oxygens on the succinimide and COO moieties, rather than an extended structure. This geometry suggests that the exposed SAM surface of **10** could be dominated by the hydrophobic aliphatic moiety rather than the hydrophilic −COO− moiety. It should be pointed out that the $\Delta(\Delta G)$ values shown here do not represent the free energy associated with adsorption onto the SAM in an absolute sense because they do not account for all of the factors in the equilibria 7 through 9. Furthermore, pK_a values are known to decrease with increasing dielectric constant of the solvent, and this could effect the parametrization.[48] Rather, the $\Delta(\Delta G)$ values provide a good measure of the relative strength of interaction between the cytochrome *c* and the layer.

Table 2. Theoretical Thermodynamic Parameters of Hydrogen-Bond (Adduct) Formation of Cytochrome *c* with Various SAMs at 298 K[a]

	ΔG_1[b]	ΔG_2[c]	$\Delta(\Delta G)$[d]
R_1−Ph (**1**)	2.5	4.2	1.9
R_1−Ph-OMe (**4**)	−0.7	2.4	0.5
R_1−Ph(CO)OMe (**5**)	−5.0	0.02	−1.4
R_1-benzodioxole (**6**)[e]	(−4.7)	(0.2)	(−1.3)
R_1−PhCN (**7**)	−5.0	0.02	−1.4
R_1−Py (**8**)	−10.3	−2.9	−3.8
R_1−PhCHO (**9**)	−5.0	0.02	−1.4
DL-thioctic-*N*-succininidyl ester[f] (**10-1**)	6.2	6.2	3.6
DL-thioctic-*N*-succininidyl ester[g] (**10-2**)	−5.8	−0.4	−1.8
DL-thioctamide[h] (**11-1**)	−12.5	−4.1	−4.7
DL-thioctamide[i] (**11-2**)	−13.3	−4.6	−5.1

[a] All values are in kJ/mol. [b] Gibbs free energy of hydrogen-bond (adduct) formation with cytochrome *c* (reference 15). [c] Gibbs free energy and enthalpy of hydrogen-bond (adduct) formation with H_2O as an acid. [d] $\Delta(\Delta G) = \Delta G_1 - \Delta G_2 - \Delta G_3$, where $\Delta G_3 = -3.6$ kJ/mol is the Gibbs free energy of hydrogen-bond (adduct) formation of cytochrome *c* with H_2O as a base, which was obtained by the parameters in Table 3. [e] The values of 1,4-dioxane estimated from Table 3. [f] The values of cycloalkanes estimated from Table 3. [g] The values of RCOOR estimated from Table 3. [h] The values of Et−NH_2 estimated from Table 3. [i] The values of $MeCONMe_2$ estimated from Table 3.

Table 3. Parameters Used by the Model of Abraham et al.[15]

acid	pK_a	$\log K_A^H$	α_2^H
lysine group	10.1[a]	1.85[b]	0.64[c]
H_2O		0.54	0.35
base		β_2^H	ln K[e]
Ph		0.14	−1.01
Ph−OMe		0.26	0.28
Ph−CO−OMe		0.42	2.01
1,4-dioxane[d]		0.41	1.90
Ph−CN		0.42	2.01
Py		0.62	4.17
Ph−CHO		0.42	2.01
cycloalkanes		0	−2.52
RCOOR		0.45	2.33
Et−NH_2		0.70	5.03
$MeCONMe_2$		0.73	5.35
H_2O		0.38	1.58

[a] This value is obtained by averaging the values of $pK_a = 9.4$ and 10.8. [b] The value of $\log K_A^H$ corresponding to $pK_a = 10.1$ was estimated from correlation of pK_a with $\log K_A^H$ in Table 3 in ref 15b. [c] The value of α_2^H was obtained using the equation $\alpha_2^H = (\log K_A^H + 1.1)/4.636$. [d] The SAM (**6**) was simulated to be 1,4-dioxane. [e] The equilibrium constant with the lysine group.

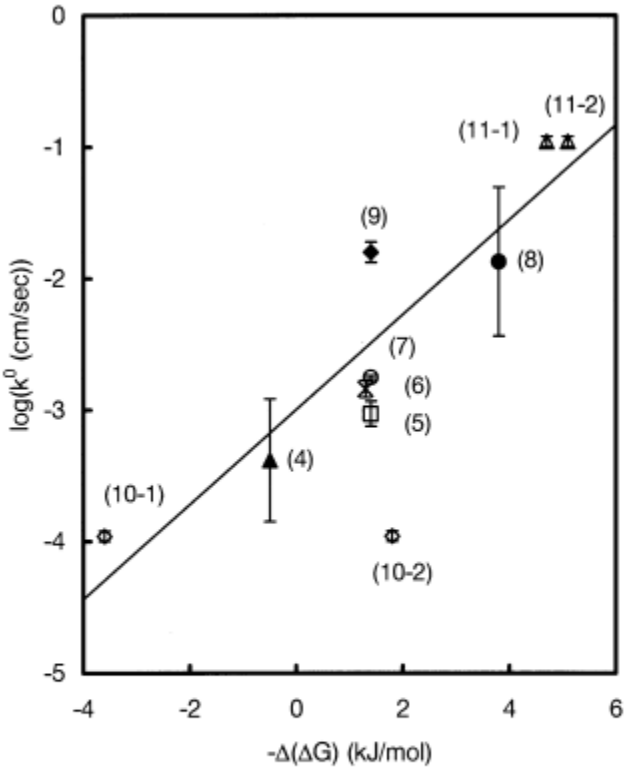

Figure 4. A plot of $\log(k^0)$ versus $-\Delta(\Delta G)$: (▲) **4**; (□) **5**; (×) **6**; (○) **7**; (●) **8**; (♦) **9**; (◊) **10**; (△) **11**. The data of **10** show the results using the parameters of the model compounds of cycloalkanes (**10-1**) and RCOOR (**10-2**). The data of **11** show the results using the parameters of the model compounds of Et−NH_2 (**11-1**) and $MeCONMe_2$ (**11-2**). A correlation factor obtained from a linear fit, excluding the point of **10-2** is 0.92.

From these discussions, it can be concluded that the 1000-fold enhancement in the electron-transfer rate constants is linked to the hydrogen bond character of the SAM surface. The change in rate constant does not appear to arise from a change in reorganization energy. In fact, a continuum model predicts a trend opposite to that needed to explain the data. Nevertheless, it is not possible to rule out some specific effect on the reorganization energy. The change in the electronic coupling with the hydrophobicity of the surface could explain the findings and could arise from at least two sources. First, the different hydrogen bonding surfaces can cause a change in the protein's orientation to the electrode and vary the tunneling distance between the heme and the electrode surface. Second, the presence of hydrogen bond interactions between the protein and the SAM, as opposed to van der Waals contacts, provides more efficient tunneling pathways between the electrode and the protein. Alternatively, the change in the apparent rate constant could arise from a change in the effective potential Φ_r at the surface, which is correlated with the change in hydrophilicity. The relative change in the hydrogen bond free energy through the series of SAMs is about 10 kJ/mol, or 0.1 eV. If all of the change in rate constant arose from this factor, it would require about two hydrogen bond interaction energies.

Summary

In summary, the electron-transfer rate constants of cytochrome *c* through 11 different SAMs on gold electrodes were observed to range from $\leq 10^{-4}$ to $\sim 10^{-1}$ cm/s. It was found that the electron transfer rate constants are strongly correlated with the Gibbs free energy of hydrogen bond adduct formation between cytochrome *c* and the SAMs. The change in the apparent standard rate constant k^0 of the cytochrome resulting from the different SAMs can be explained by changes in the electronic coupling and the effective potential near the surface.

Acknowledgment

We thank BSF and NSF for support of this work.

References

1. (a) Durham, B.; Millet, F. S. Iron: Heme Proteins & Electron Transport. In *Encyclopedia of Inorganic Chemistry*; King, R. B., Ed.; John Wiley & Sons: New York, 1994; Vol. 4, pp 1642−1661. (b) Gray, H. B.; Winkler, J. R. *Annu. Rev. Biochem.* **1996**, *65*, 537.
2. (a) Barker, S. L. R.; Clark, H. A.; Swallen, S. F.; Kopelman, R.; Tsang, A. W.; Swanson, J. A. *Anal. Chem.***1999**, *71* (9), 1767.
3. (a) Rusling, J. F. *Interface* **1997**, *6* (4), 26. (b) Taniguchi, I. *Interface* **1997**, *6* (4), 34. (c) Zhou, Y.; Nagaoka, T.; Zhu, G. *Biophys. Chem.* **1999**, *79*, 55. (d) Bowden, E. F. *Interface***1997**, *6* (4), 40.
4. (a) Taniguchi, I.; Toyosawa, K.; Yamaguchi, H.; Yasukouchi, K. *J. Electroanal. Chem.* **1982**, *140*, 187. (b) Haladjian, J.; Bianco, P.; Pilard, R. *Electrochim. Acta* **1983**, *28*, 1823.
5. (a) Allen, P. M.; Hill, H. A. O.; Walton, N. J. *J. Electroanal. Chem.* **1984**, *178*, 69. (b) Hill, H. A. O.; Page, D. J.; Walton, N. J.; Whitford, D. *J. Electroanal. Chem.* **1985**, *187*, 315. (c) Hill, H. A. O.; Page, D. J.; Walton, N. J. *J. Electroanal. Chem.* **1986**, *208*, 395.

(d) Armstrong, F. A.; Hill, H. A. O.; Walton, N. J. *Acc. Chem. Res.* **1988**, *21*, 407. (e) Armstrong, F. A. *Struct. Bond.* **1990**, *72*, 137. (f) Hill, H. A. O.; Hunt, N. I. *Methods in Enzymology*: *Metallobiochemistry*; Riordan, J. F., Vallee, B. L., Eds.; Academic Press: New York, 1993; Vol. 227, p 501.

6. (a) Bond, A. M. *Inorg. Chim. Acta* **1994**, *226*, 293. (b) Ruzgas, T.; Wong, L.; Gaigalas, A. K.; Vilker, V. L. *Langmuir* **1998**, *14*, 7298.
7. (a) Finklea, H. O. *Electroanalytical. Chemistry*; Bard, A. J., Ed.; Dekker: New York, 1996; Vol. 19, p 109. (b) Smalley, J. F.; Feldberg, S. W.; Chidsey, C. E. D.; Linford, M. R.; Newton, M. D.; Liu, Y.-P. *J. Phys. Chem.* **1995**, *99*, 13141. (c) Weber, K.; Hockett, L.; Creager, S. *J. Phys. Chem. B***1997**, 8286.
8. Beratan, D. N.; Betts, J. N.; Onuchic, J. N. *Science* **1991**, *252*, 1285.
9. Lay, P. A. *J. Phys. Chem.* **1986**, *90*, 878. The formal potential E_f is expressed by the following equation where E_f^0 is the hypothetical solvent-free redox potential, ΔE_p is the shift by the solvent dipoles, ΔE_{int} is the shift by the differing effect of the two oxidation states of redox couple on the solvent structure, and ΔE_H is the shift by the interactions between the solvent and the redox couple involving hydrogen bond interactions, π−π interactions, and direct bonding interactions.
10. (a) Decornez, H.; H−Schiffer, S. *J. Phys. Chem. A* **2000**, *104*, 9370. (b) Turró, C.; Chang, C. K.; Leroi, G. E.; Cukier, R. I.; Nocera, D. G. *J. Am. Chem. Soc.* **1992**, *104*, 4013. (c) Myles, A. J.; Branda, N. R. *J. Am. Chem. Soc.* **2001**, *123*, 177.
11. (a) Napper, A. M.; Read, I.; Waldeck, D. H.; Head, N. J.; Oliver, A. M.; Paddon-Row, M. N. *J. Am. Chem. Soc.* **2000**, *122*, 5220. (b) Kumar, K.; Lin, Z.; Waldeck, D. H.; Zimmt, M. B. *J. Am. Chem. Soc.* **1996**, *118*, 243. (c) Read, I.; Napper, A. M.; Zimmt, M. B.; Waldeck, D. H. *J. Phys. Chem.* **2000**, *104*, 9385.
12. (a) Finklea, H. O.; Liu, L.; Ravenscroft, M. S.; Punturi, S. *J. Phys. Chem.* **1996**, *100*, 18852. (b) Sumner, J. J.; Weber, K. S.; Hockett, L. A.; Creager, S. E. *J. Phys. Chem. B* **2000**, *104*, 7449. (c) Napper, A. M.; Liu, H.; Waldeck, D. H. *J. Phys. Chem. B* **2001**, *105*, 7699. (d) Cheng, J.; Saghi-Szabo, G.; Tossell, J. A.; Miller, C. J. *J. Am. Chem. Soc.* **1996**, *118*, 680.
13. (a) Yamamoto, H.; Waldeck, D. H. *J. Phys. Chem. B* **2002**, *106*, 7469. (b) Slowinski, K.; Chamberlain, R. V.; Miller, C. J.; Majda, M, *J. Am. Chem. Soc.* **1997**, *119*, 11910.
14. Niki, K.; Pressler, K. R.; Sprinkle, J. R.; Li, H.; Margoliash, E. *Russ. J. Electrochem.* **2002**, *38*, 63.
15. (a) Abraham, M. H.; Grellier, P. L.; Prior, D. V.; Taft, R. W.; Morris, J. J.; Taylor, P. J.; Laurence, C.; Berthelot, M.; Doherty, R. M.; Kamlet, M. J.; Abboud, J.-L. M.; Sraidi, K.; Guihéneuf, G. *J. Am. Chem. Soc*. **1988**, *110*, 8534. (b) Abraham, M. H.; Grellier, P. L.; Prior, D. V.; Morris, J. J.; Taylor, P. J. *J. Chem. Soc., Perkin Trans. 2* **1990**, 521. (c) Abraham, M. H.; Grellier, P. L.; Prior, D. V.; Duce, P. P.; Morris, J. J.; Taylor, P. J. *J. Chem. Soc., Perkin Trans. 2* **1989**, 699. (d) Abraham, M. H.; Duce, P. P.; Prior, D. V.; Barratt, D. G.; Morris, J. J.; Taylor, P. J. *J. Chem. Soc., Perkin Trans. 2* **1989**, 1355.
16. Brutigan, D. L.; Ferguson, S.; Margoliash, E. *Methods in Enzymology*; Fleischer, S., Packer, L., Ed.; Academic Press: New York, 1978; Vol. 53, p 131.

17. Yamamoto, H.; Liu, H.; Waldeck, D. H. *Chem. Commun.* **2001**, 1032. See Supporting Information.
18. Blonder, R.; Willner, I.; Bückmann, A. F. *J. Am. Chem. Soc.* **1998**, *120*, 9335.
19. Ulman *Chem. Rev.* **1996**, *96*, 1533.
20. Terrettaz, S.; Cheng, J.; Miller, C. J.; Guiles, R. D. *J. Am. Chem. Soc*. **1996**, *118*, 7857.
21. (a) Tarlov, M. J.; Bowden, E. F. *J. Am. Chem. Soc*. **1991**, *113*, 1847. (b) Collinson, M.; Bowden, E. F.; Tarlov, M. J. *Langmuir* **1992**, *8*, 1247. (c) Song, S.; Clark, R. A.; Bowden, E. F.; Tarlov, M. J. *J. Phys. Chem.* **1993**, *97*, 6564. (d) Bowden, E. F.*Interface* **1997**, *6*, 40. (e) Clark, R. A.; Bowden, E. F. *Langmuir* **1997**, *13*, 559.
22. (a) Eddowes, M. J.; Hill, H. A. O. *J.* Chem. Soc., *Chem. Commun.* **1977**, 771. (b) Eddowes, M. J.; Hill, H. A. O. *J. Am. Chem. Soc.* **1979**, *101*, 4461. (c) Taniguchi, I.; Toyosawa, K.; Yamaguchi, H.; Yasukouchi, K. *J.* Chem. Soc., *Chem. Commun.* **1982**, 1032.
23. Sivakolundu, S. G.; Mabrouk, P. A. *J. Am. Chem. Soc.* **2000**, *122*, 1513.
24. Chen, X.; Ferrigno, R.; Yang, J.; Whitesides, G. M. *Langmuir*, **2002**, *18*, 7009.
25. Rivas, L.; Murgida, D. H.; Hildebrandt, P. J. *Phys. Chem. B* **2002**, *106*, 4823.
26. (a) Bard, A. J.; Faulkner, L. R. *Electrochemical Methods*, 2nd ed.; John Wiley & Sons: New York, 2000; pp 218−223. The peak currents I_p and potentials E_p in the reversible and irreversible system are given by the following equations: (1) The reversible system and (2) The irreversible system and where E_p is a peak potential (V), $E^{0\text{‘}}$ is a formal potential (V), α is the transfer coefficient, n is the number of electrons per molecule oxidized or reduced, n_a is the number of electrons involved in the rate-determining step, D_O and D_R are the diffusion constants (cm^2/s) for oxidized and reduced species, v is the scan rate (V/s), A is the electrode area (cm^2), C_0* is the concentration in the bulk solution (mol/cm^3), and R, T, and F are the gas constant, the temperature, and the Faraday constant, respectively. In the present case, the area A is 0.1 cm^2, the scan rate is 20 mV/s, the diffusion constant of horse cytochrome *c* is 4.7×10^{-7} cm^2/s (ref 20), and the concentration of cytochrome *c* is 50 μM (=0.050 $\mu mol/cm^3$). (3) the work term comes from the interaction of SAM with + − both O and R states of redox species. (b) Bard, A. J.; Faulkner, L. R. *Electrochemical Methods*, 2nd ed.; John Wiley & Sons: New York, 2000; pp 224−231. (c) H. Matsuda, Y.; Ayabe, *Z. Elektrochem.* **1955**, *59*, 494.
27. If $\Lambda \geq 10$, the peak behaves like a reversible system, in which I_p is proportional to the $v^{1/2}$, and the value of $|E_p - E_{p/2}|$ is expected to be close to 56.5 mV at 25 °C. For $0.1 \leq \Lambda \leq 10$, the system is quasi-reversible and one expects to see some deviation from the ideal response. If $\Lambda \leq 0.1$, I_p is not proportional to the $v^{1/2}$, and the value of $|E_p - E_{p/2}|$ should be more than 56.5 mV.
28. Nicholson, R. S. *Anal. Chem*. **1965**, *37*, 1351.
29. Matsuda and Ayabe suggested the quasi-reversible zone in terms of the electron-transfer rate constant with the scan rate v to be $0.3v^{1/2} \geq k^0 \geq 2 \times 10^{-5}v^{1/2}$.[26b,c] According to this zone, the electron-transfer reactions in the systems of **4**−**10** at v = 20 mV/s are quasi-reversible, while that of **11** is reversible.
30. Weber, K.; Creager, S. E. *Anal. Chem*. **1994**, *66*, 3164.
31. Honeychurch, M. J.; Rechnitz, G. A. *J. Phys. Chem. B* **1997**, *101*, 7472.

32. (a) Khoshtariya, D. E.; Dolidze, T. D.; Zusman, L. D.; Waldeck, D. H. *J. Phys. Chem. A* **2001**, *105*, 1818. (b) Khoshtariya, D. E.; Wei, J.; Yamamoto, H.; Liu, H.; Dick, A.; Waldeck, D. H.*Angew. Chem.* **2002**, *41*, 4700. (c) Wei, J.; Yamamoto, H.; Liu, H.; Dick, A.; He, Y.; Waldeck, D. H. *J. Am. Chem. Soc.* **2002**, *124*, 9591. The electron-transfer distance in the intermediate regime between the adiabatic and nonadiabatic limits is reported to be 15−20 Å.
33. Sachs, S. B.; Dudek, S. P.; Hsung, R. P.; Sita, L. R.; Smalley, J. F.; Newton, M. D.; Feldberg, S. W.; Chidsey, C. E. D. *J. Am. Chem. Soc.* **1997**, *119*, 10563.
34. (a) McLendon, G.; Pardue, K.; Bak, P. P. *J. Am. Chem. Soc.* **1987**, *109*, 7540. (b) Graige, M. S.; Feher, G.; Okamura, M. Y. *Proc. Natl. Acad. Sci. U.S.A.* **1998**, *95*, 11679. (c) Davidson, V. *Biochemistry* **2000**, *39*, 4924. (d) Davidson, V.*Acc. Chem. Res.* **2000**, *33*, 87.
35. (a) Feng, Z. Q.; Imabayashi, S.; Kakuichi, T.; Niki, K. *J. Chem. Soc., Faraday Trans.* **1997**, *93*, 1367. (b) Avila, A.; Gregory, B. W.; Niki, K.; Cotton, T. M. *J. Phys. Chem. B* **2000**, *104*, 2759.
36. (a) Mikkelsen, K. V.; Ratner, M. A. *Chem. Rev.* **1987**, *87*, 113. (b) Barbara, P. F.; Meyer, T. J.; Ratner, M. A. *J. Phys. Chem.* **1996**, *100*, 13148.
37. (a) Newton, M. D.; Friedman, H. L. *J. Chem. Phys.* **1985**, *83*, 5210; (b) Gochev, A.; McManis, G. E.; Weaver, M. J. *J. Chem. Phys.* **1989**, *91*, 906.
38. By assuming a simple Arrhenius form for the apparent standard rate constant with *A* constant between systems with different SAMs, one can determine the change in activation energy that is required to reproduce the data, i.e., For the 1000-fold rate constant change between SAMs **10** and **11**, the difference of activation energy is 0.198 eV.
39. Sigfridsson, E.; Olsson, M. H. M.; Ryde, U. *J. Phys. Chem. B* **2001**, *105*, 5546.
40. Marcus, R. A. *J. Chem. Phys.* **1965**, *43*, 679.
41. (a) Zhang, X.; Esenturk, O.; Walker, R. A. *J. Am. Chem. Soc.* **2001**, *123*, 10768. (b) Zhang, X.; Walker, R. A. *Langmuir* **2001**, *17*, 4486. (c) Wang, H.; Borguet, E.; Eisenthal, K. B. *J. Phys. Chem. B* **1998**, *102*, 4927. (d) Miranda, P. B.; Pflumio, V.; Saijo, H.; Shen, Y. R. *J. Am. Chem. Soc.* **1998**, *120*, 12092. (e) Lum, K.; Chandler, D.; Weeks, J. D. *J. Phys. Chem. B* **1999**, *103*, 4570.
42. Liu, Y.-P.; Newton, M. D. *J. Phys. Chem.* **1994**, *98*, 7162. The solvent reorganization energy λ_s is given by the following equation; where *a* is the cavity radius of the redox species, *d* is the distance from the redox species to the top of a film on the electrode, *L* is the film thickness, and $\Delta q = \pm 1$ for a point charge. ε is the dielectric constant, where the superscripts of op and st mean optical and static, and the subscripts I, II, III mean the bulk solvent, the film, and the electrode, respectively. The parameters are set up, as follows: L = 12 Å, $a = d$ = 5 Å, ε_I^{st} = 50 and 120, ε_I^{op} = 1.8, $\varepsilon_{II}^{st} = \varepsilon_{II}^{op}$ = 2.25, $\varepsilon_{III}^{st} = \varepsilon_{III}^{op} = \infty$.
43. *CRC Handbook of Chemistry and Physics*; Lide, D. R., Ed.; CRC: Boca Raton, Ann Arbor, London, Tokyo, 1994.
44. Beratan, D. N.; Bettis, J. N.; Onuchic, J. N. *Science* **1991**, *252*, 1285.

45. (a) Sek, S.; Misicka, A.; Bilewicz, R. *J. Phys. Chem. B* **2000**, *104*, 5399. (b) Sek, S.; Bilewicz, R. *J. Electroanal. Chem*. **2001**, *509*, 11.
46. These distances were obtained using The Protein Data Bank: Berman, H. M.; Westbrook, J.; Feng, Z.; Gilliland, G.; Bhat, T. N.; Weissig, H.; Shindyalov, I. N.; Bourne, P. E. *Nucleic Acids Res.* **2000**, *28*, 235.http://www.rcsb.org/pdb/.
47. Millett, F.; Durham, B. *Cytochrome c*; Scott, R. A., Mauk, A. G., Eds.; University Science Books: Sausalito, CA, 1996; p 595.
48. Perrin, D. D.; Dempsey, B.; Serjeant, E. P. *pK*$_a$ *Prediction for Organic Acids and Bases*; Chapman and Hall: New York, 1981.

Supplemental Information

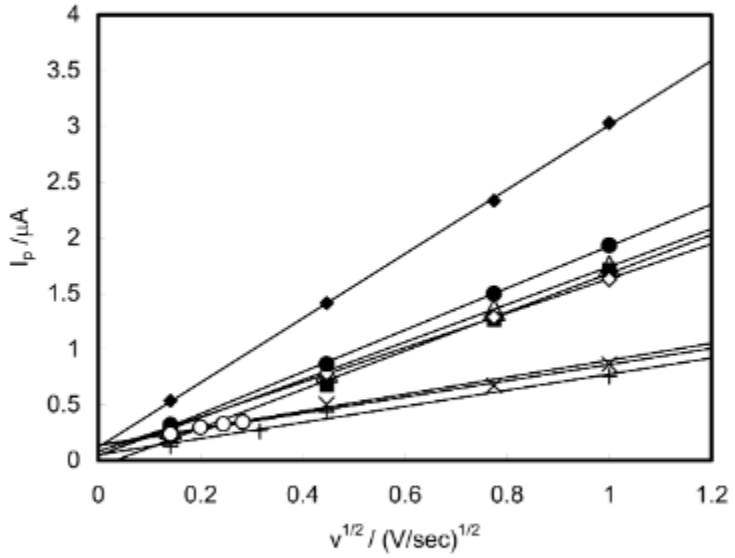

Figure A. A plot of I_p vs the square root of the scan rate: The SAMs of **(4)** filled squares; **(5)** x; **(6)** open triangles; **(7)** open diamonds; **(8)** +; **(9)** filled circles; **(10)** open circles; **(11)** filled diamonds. The data of **(4)** to **(9)**, and **(11)** were measured from the oxidation peaks, while the data of **(10)** were taken from the reduction peaks. See the details in the text.